Journal of Cellular Biochemistry Supplement 34:67–72 (2000)

Endpoint Markers for Cancer Chemoprevention Trials Derived From the Lesion of Precancer (Intraepithelial Neoplasia) Measured by Computer-Assisted Quantitative Image Analysis

Charles W. Boone* and Gary J. Kelloff

Division of Cancer Prevention, National Cancer Institute, National Institutes of Health, Bethesda, Maryland 20892

Abstract Endpoint markers for cancer chemoprevention clinical trials are described that are developed from the morphological properties of the precancerous lesion of intraepithelial neoplasia itself, as measured by computer-assisted quantitative image analysis. The markers include increased proliferative fraction (percentage MIB-1 positive nuclear area); nuclear DNA content (DNA ploidy), including DNA content exceeding fivefold the haploid amount (5C-exceeding rate); nuclear/nucleolar morphometry; and disorganization of nuclear chromatin pattern as characterized by Markovian parameters and other functions. A significant new advance in image analysis is the process of "tiling," in which hundreds of full monitor image fields of a given histological section at ×40 magnification are reduced in size and fused seamlessly to produce a single image of the histological section at ×1.25 magnification. The operator may review the low-power image and retrieve ×40 magnification of any desired area by point/clicking with a mouse. J. Cell. Biochem. Suppl. 34:67–72, 2000. Published 2000 Wiley-Liss, Inc.†

Key words: endpoint markers; chemoprevention trials; computer-assisted image analysis

With few exceptions, the microscopic diagnosis of cancer, as applied to epithelia, depends on the finding of an intraepithelial neoplastic lesion which is invasive across the basement membrane. As illustrated in Figure 1, the requirement that invasiveness be present in order to make the diagnosis of cancer serves to orient the nomenclature of neoplastic progression into terms describing two consecutive neoplastic stages that differ from each other only by the property of invasiveness. The first stage is termed preinvasive neoplasia, premalignancy, precancer, intraepithelial neoplasia, or dysplasia, and the second lesion is termed invasive neoplasia, malignancy, or cancer. The Chemoprevention Program at the National Cancer Institute (NCI) is sponsoring a large number of clinical trials testing cancer chemopreventive agents for their efficacy in causing preinvasive, intraepithelial neoplastic lesions to regress, remain stationary, or at least progress more slowly to an invasive lesion.

The focus of this article is on the description of endpoint markers for chemoprevention trials that are from the morphological properties of the precancerous lesion of intraepithelial neoplasia itself, as measured by computer-assisted image analysis. The list of morphologic criteria by which the diagnosis of intraepithelial neoplasia is made have been reviewed previously [Boone and Kelloff, 1992]. Briefly, they are increased proliferative fraction (percentage of cycling cells), increased nuclear size, abnormal nuclear shape, disorganization of nuclear chromatin pattern, abnormal mitoses (e.g., tripolar mitosis, anaphase chromosome lagging), and abnormal or absent maturation. In glandular epithelia, such as breast and prostate, an additional criterion is the presence of an increased number of nucleoli showing enlargement and abnormal shape.

*Correspondence to: Charles W. Boone, 6130 Executive Blvd, Rockville MD 20815.

Received 15 October 1998; Accepted 9 March 1999

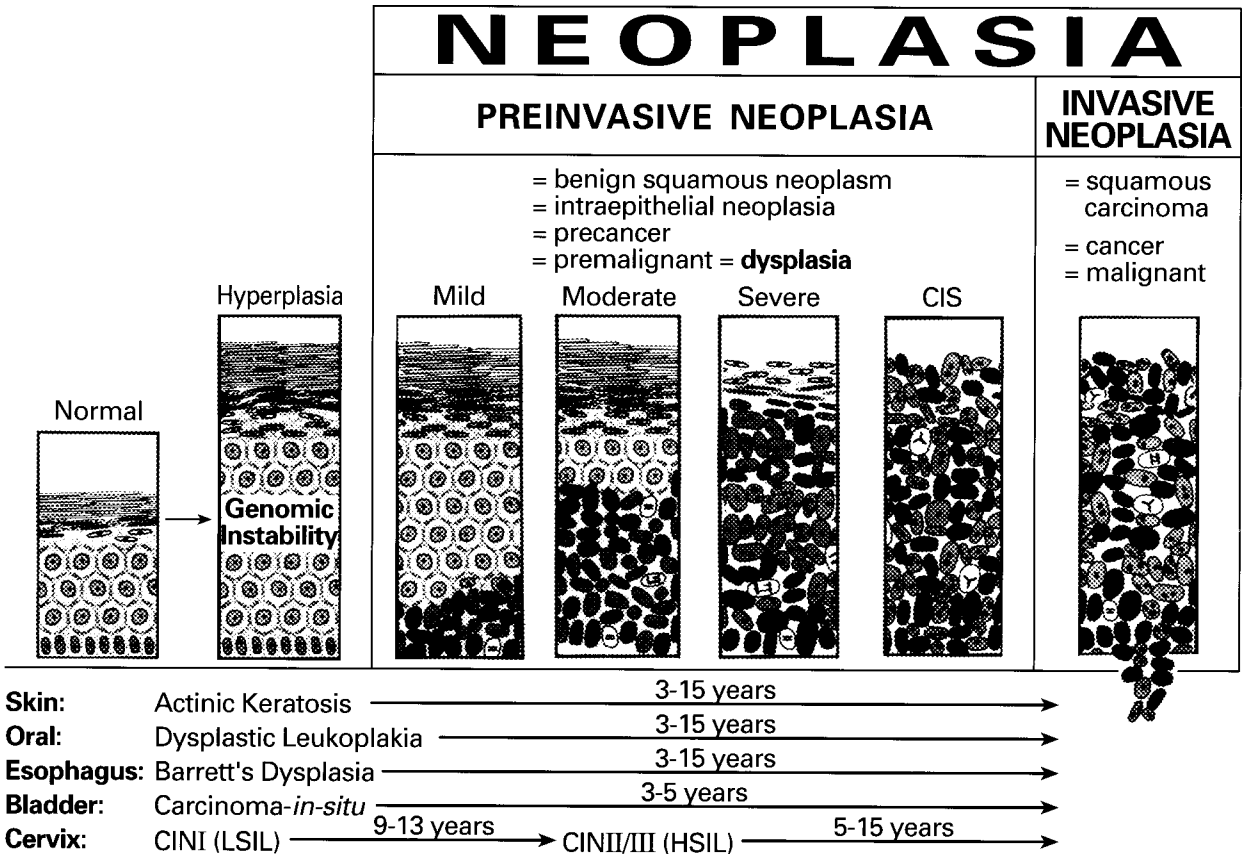

Fig. 1. Diagramatic representation of neoplasia of squamous epithelium, preceded by hyperplasia and genomic instability. The nomenclature of neoplastic progression describes essentially two neoplastic lesions, which follow each other in time. The first lesion is termed preinvasive neoplasia, precancer, premalignancy, intraepithelial neoplasia, or dysplasia; the second lesion, defined by invasiveness across the basement membrane, is termed invasive neoplasia, malignancy, or cancer. CIS, carcinoma in situ; CIN, cervical intraepithelial neoplasia; LSIL, HSIL, low-grade and high-grade squamous intraepithelial lesion.

Table I lists clinical trials in the Chemoprevention Program that use computer-assisted image analysis of tissue biopsies and/or cytological smears as endpoint markers. Thirteen of the trials are testing the efficacy of the candidate chemopreventive agents listed; the other two are developing more precise and predictive endpoint markers. In these and other clinical trials sponsored by the Chemoprevention Branch, a number of additional molecular endpoint markers are also being used.

Table I shows the variety of imaging equipment being used in the clinical trials. The BLISS instrument is an advanced version of the CAS 200 instrument. In each of the clinical trials, the core image analysis measurements may be summarized as proliferative fraction, nuclear DNA content (DNA ploidy), nuclear morphometry (nuclear/nucleolar size, shape, and extent of variation of size and shape), and nuclear chromatin texture.

IMAGE ANALYSIS MEASUREMENTS

Proliferative Fraction

A preferred antibody probe for measuring cellular proliferation rate is MIB-1, which can be used on formalin-fixed tissue and developed with a chromogen-bearing conjugate. The computer identifies the total area of nuclei bound to the MIB-1 antibody and expresses this as the percentage of total nuclear area that is antibody positive, termed percentage positive nuclear area (PPNA).

Nuclear DNA Content (DNA Ploidy)

The DNA index, a common measure of DNA ploidy, is a frequency histogram of epithelial cell nuclear DNA content referenced to a nor-

TABLE I. Institutions, Target Cohorts, Chemopreventive Agents, and Imaging Equipment Used for Quantitative Measurement of Clinical Trial Endpoints

INSTITUTION	ORGAN/LESION	CHEMOPREVENTIVE AGENT	ENDPOINT IMAGING EQUIPMENT
Kansas U. Medical Center	Breast/DCIS	DFMO	BLISS (Bacus Labs)
MD Anderson Cancer Center	Breast/DCIS	4-HPR + Tamoxifen	Cyto-Savant (Xyllix)
Georgetown U. Medical Center	Breast/DCIS	Exemestane	Samba 4000
U. Alabama	Cervix/CIN	9-cis-Retinoic Acid	BLISS (Bacus Labs)
U. Alabama	Prostate/PIN	DFMO	Cyto-Savant (Xyllix)
U. Alabama	Prostate/PIN	4-HPR	Cyto-Savant (Xyllix)
U. Michigan	Prostate/PIN	Se-Enriched Yeast	BLISS (Bacus Labs)
U. Oklahoma	Bladder/TaT1 TIS	4-HPR	CAS 200 (Becton-Dickinson)
U. Calif. Irvine	Colon/Adenoma	DFMO + Sulindac	CAS 200 (Becton-Dickinson)
New York U. Medical Center	Colon/Adenoma	$CaCO_3$ + VIT D3	Samba 4000
New York U. Medical Center	Color/Adenoma	Sulindac	Samba 4000
Fox Chase Cancer Center	Oral Cavity/Leukoplakia	DFMO	Roche Workstation
U. Michigan	Barrett Esophagus	DFMO	Roche Workstation
U. Texas SW Medical Center	Lung/dysplasia	Anethole Trithione	Cyto-Savant (Xyllix)
Fox Chase Cancer Center	Lung/dysplasia	Oltipraz	Roche Workstation

DCIS, ductal carcinoma in situ; 4-HPR, 4-hydroxyphenylretinamide; CIN, cervical intraepithelial neoplasia; PIN, prostatic intraepithelial neoplasia; TaT1, grades of superficial bladder neoplasia; TIS, bladder carcinoma in situ; DFMO, difluoromethylornithine;

mal diploid cell population in the same tissue such as stromal fibroblasts or lymphocytes. In this system, diploid epithelial cells have a DNA index of 2.0. In histological sections, cell nuclei are frequently truncated by the microtome knife, giving artifactually low values for nuclear DNA content. To control for nuclear truncation error, a piece of rodent liver of accurately known nuclear DNA content is used as a reference. On the other hand, intact uncut epithelial cell nuclei are obtained from smears of cells that have been brushed or scraped from an epithelium, or have naturally exfoliated. Protease-disaggregated core biopsies of the breast also yield uncut nuclei.

Associated with the nuclear DNA frequency histogram are numerous parameters that have been standardized by an international conference [Bocking et al., 1995]. An example of a parameter that has been used to predict clinical outcome is the 5c exceeding rate (5cER), or the percentage of cells with nuclear DNA content that exceeds fivefold the haploid amount of nuclear DNA. This parameter was first introduced by Bocking et al. [1984] and has been recently used as a predictor for the outcome of urological neoplasia by Hemstreet et al. [1991]. DNA aneuploidy has been shown to occur during the preinvasive phase of neoplastic progression (intraepithelial neoplasia) in bladder, prostate, breast, cervix, skin, oral leukoplakia, larynx, lung, esophagus, stomach, and colorectum (reviewed by Boone and Kelloff, [1992].

Nuclear Morphometry

The hallmark morphologic changes of neoplasia are abnormally increased nuclear size, abnormally altered nuclear shape (measured by various roundness factors), and pleomorphism of size and shape (related to increased variance of size and shape) [Boone and Kelloff, 1993]. Nucleoli are ribosome factories expressed by genes located on the acrocentric chromosomes 13–15, 21, and 22 [Alberts et al., 1989]. Changes in nuclear morphometry have been reported to be a correlate of the extent of neoplastic progression in prostatic intraepithelial neoplasia [Montironi et al., 1991]. Argyrophilic nucleolar organizer region-associated proteins are found within nucleoli and form the basis for the Ag-NOR stain. Using this stain, the number of nucleolar organizer regions (NORs) clearly distinguished between tubular adenomas, villous adenomas with moderate versus severe nuclear atypia, and colorectal adenocarcinoma [Yang et al., 1990].

Abnormal Nuclear Chromatin Texture

The development of neoplastic change is frequently associated with aberrations and incom-

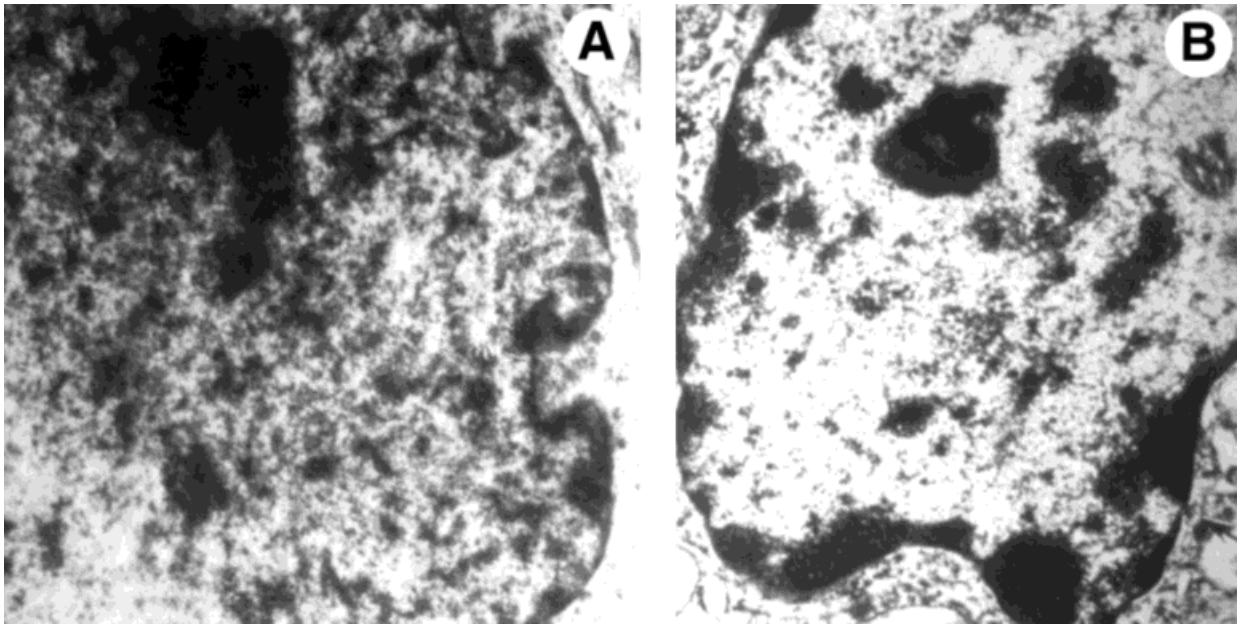

Fig. 2. Low-power electron micrographs of cell nuclei from the uterine cervix. **A:** Nucleus of a hyperplastic normal cell. **B:** Nucleus of a cell from a lesion of cervical intraepithelial neoplasia. Note the diagnostic feature of coarse chromatin clumping with sharply marginated borders. The computer detects this sharp margination by the "deep valley" algorithm (see text).

pleteness of differentiation of specialized cellular structures. This failure of phenotypic differentiation is a reflection of the failure of the DNA segments that code for them to decondense in preparation for transcription of messenger RNA. These regions of nondecondensed DNA are seen by the image analyzer as regions of increased granularity of nuclear chromatin texture. Later during the process of neoplastic progression, the progressive increase in granularity is extensive enough to be seen visually under the microscope, consisting of abnormally coarse clumps that are a diagnostic feature of neoplasia.

Markovian analysis is commonly applied to the nuclear chromatin texture of DNA-stained cells [Pressman, 1976]. The computer-assisted image analyzer divides the image of the nucleus into rectangular picture elements, or "pixels," averaging 0.67 μm on a side. The optical density of light transmitted through each pixel depends on the mass of stained DNA in its the light path. Thus, the computer views chromatin texture as a field of pixel optical densities. Each individual nucleus has a unique pattern of pixel optical densities that may be described by some 21 Markov texture parameters and other functions. If the computer is trained on a known teaching set of neoplastic nuclei to obtain the most predictive Markov parameters, a test set of unknown nuclei may be discriminated with high rates of correct classification between images of normal versus neoplastic cell nuclei [Pressman, 1976].

DEEP VALLEY DETECTOR, AN ALGORITHM THAT DETECTS NUCLEAR TEXTURE FEATURES SPECIFIC FOR NEOPLASIA

Abnormally clumped nuclear chromatin showing sharply defined and angulated borders is a well-established morphologic characteristic of neoplastic change. Figure 2 compares the nuclear chromatin pattern of a normal hyperplastic cell from the uterine cervix with the chromatin pattern of a neoplastic cell the lesion of cervical intraepithelial neoplasia in the same tissue. The large chromatin clumps with sharply marginated and angulated borders in the neoplastic nucleus are easily seen. In addition, the thickening of the nuclear membrane caused by attached clumps of sharply marginated chromatin is another characteristic of neoplastic change. To measure these neoplasia-specific changes in nuclear chromatin, a software program was designed which detects sites in the nucleus having a steep optical density dropoff, such as those at the sharply defined borders of chromatin clumps [Boone and Kelloff, 1998]. In one study, neoplastic cells of the uterine cervix averaged more than 100 deep valley sites per

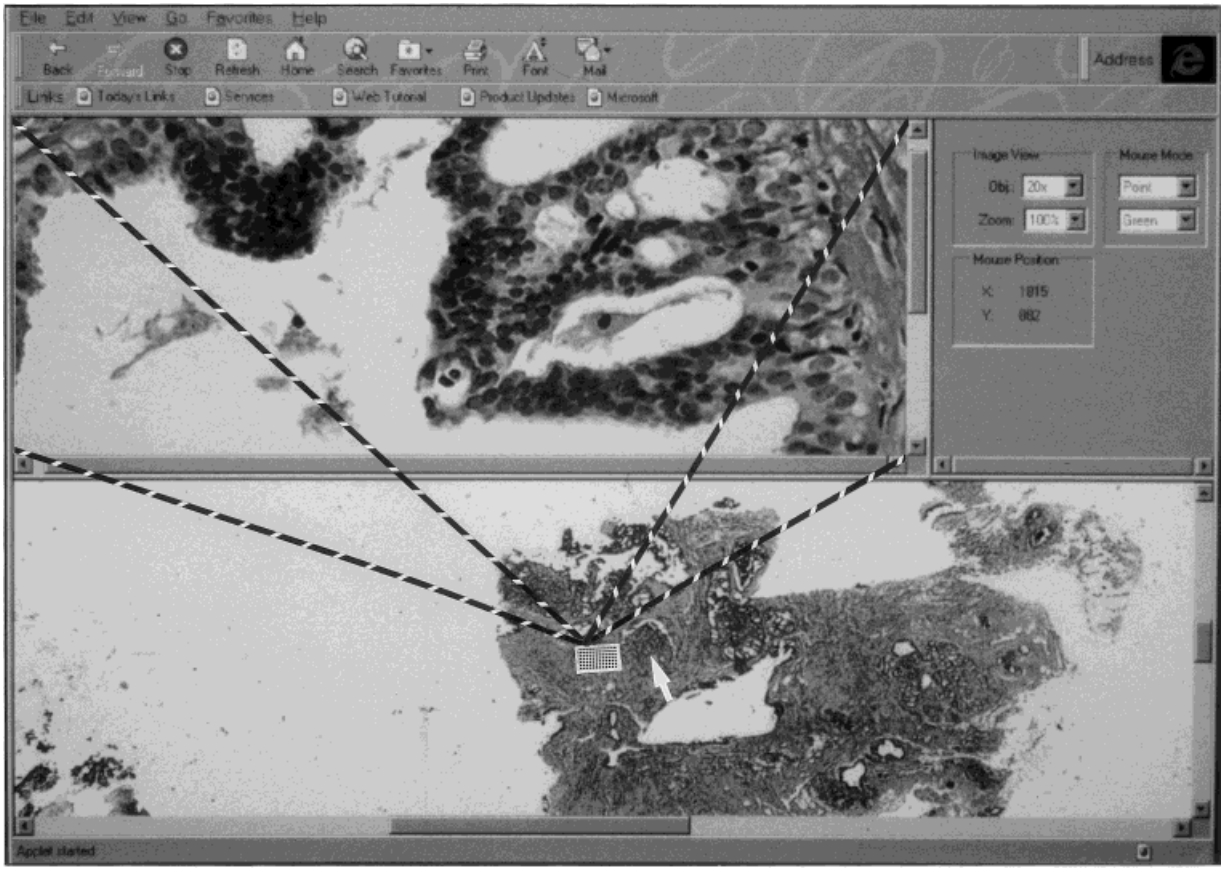

Fig. 3. Video monitor image that appears during the tiling process. The bottom image shows a histological section of human breast ductal carcinoma in situ at ×1.25 magnification, which has been previously tiled (see text). The white arrow is the mouse point/click setting that produced the top image at ×20 magnification. The top image shows the classic tissue pattern of Roman bridging, which is a diagnostic feature of breast ductal carcinoma in situ.-

nucleus, as compared with less than 20 deep valley sites per nucleus of normal hyperplastic cervical cells.

TILING, A SIGNIFICANT NEW ADVANCE IN IMAGE ANALYSIS

In the past, a major drawback in the application of computer-assisted image analysis to histologic sections has been the inability of the computer to analyze more than one small portion of the histologic image at a time. Randomly selected portions of the image must be analyzed serially in order to build up an evaluation of the complete histological section. Recently the problem of limited image area per view has been solved by a newly developed algorithm called "tiling" (a feature of the BLISS instrument made by Bacus Laboratories, Inc.). The tiling process starts with the registration on the full monitor screen of a microscopic image field at ×40 magnification, covering a real area of tissue on the histological slide of approximately 170 × 280 µm. The ×40 field is reduced in size by the computer to a small rectangular area, or tile, measuring only approximately 1 × 1.75 µm on the monitor screen. The computer moves to the adjacent image field at ×40 magnification and repeats the size reduction to a tile adjacent to the initial one. The process is repeated until the entire histological section scanned across many views at ×40 has been reduced to a single image of the entire tissue section appearing on the same monitor screen at ×1.25, made up of hundreds of tiles seamlessly fused together. Each tile still has the information originally obtained at ×40, so that at any time the viewer may place the mouse pointer over a desired portion of the low-power image and click to view this portion again at ×40 magnification.

In summary, the tiling system allows the operator first to view the entire histological section at low power and then to "point and

click" with the mouse to view desired portions of the histological section at ×20 or ×40 magnification. Figure 3 shows the video monitor image as viewed during the tiling process. The monitor image is split horizontally into two panels. The lower panel shows a histological section of human breast ductal carcinoma in situ at ×1.25 magnification, which has been previously tiled. The white arrow is the mouse point/click setting which produced the upper panel image at ×20 magnification. Both the lower and upper panels have extended areas that may be brought into view by using the mouse to operate the vertical and horizontal scroll bars seen at the sides of the images. The upper panel image at ×20 shows the classic tissue pattern of "Roman bridges," a diagnostic feature of breast ductal carcinoma in situ (DCIS).

REAL-TIME REMOTE MICROSCOPY OVER THE INTERNET

An operator at a remote site using an ordinary mouse-controlled PC may download from an internet address a microscopic image such as the one in the lower panel of Figure 3. This real-time video image is produced by the BLISS instrument as it scans a histological slide under the microscope. The remote operator may control the mechanical stage of the microscope using only his mouse to point/click on a desired area of the histological section he wishes to view at ×20 or ×40 magnification. Any number of additional operators at remote sites may view the same image simultaneously, using their mouse pointers to indicate various aspects of the histological image as they converse by conference telephone.

REFERENCES

Alberts B, Bray D, Lewis J, Raff M, Roberts K, Watson JD. 1989. Molecular biology of the cell. 2nd Ed. New York: Garland. p 541–544.

Bocking A, Adler CP, Common HH, Hilgarth HM, Granzen B, Aufferman WW. 1984. Algorithm for a DNA cytometric diagnosis and grading of malignancy. Anal Quant Cytol 6:1–8.

Bocking A, Giroud F, Reith A. 1995. Consensus report of the European Society for Analytical Cellular Pathology Task Force on Standardization of Diagnostic DNA Image Cytometry. Anal Quant Cytol Histol 17:1–7.

Boone CW, Kelloff GJ. 1992. Natural history of intraepithelial neoplasia in humans with implications for cancer chemoprevention strategy. Cancer Res 52:1651–1659.

Boone CW, Kelloff GJ. 1993. Intraepithelial neoplasia, surrogate endpoint biomarkers, and cancer chemoprevention. J Cell Biochem Suppl 17F:37–48.

Boone CW, Kelloff GJ. 1998. Endpoint markers for clinical trials of chemopreventive agents derived from the properties of epithelial precancer (intraepithelial neoplasia) measured by computer-assisted image analysis. In: Ponten J, editor. Precancer biology, importance and possible prevention. Cancer surveys. Vol 32. p 133–147.

Hemstreet GP III, Rollins S, Jones P, Rao JY, Hurst RE, Bonner RB, Hewett T, Smith BG. 1991. Identification of a high risk subgroup of grade 1 transitional cell carcinoma using image analysis based deoxyribonucleic acid ploidy analysis of tumor tissue. J Urol 146:1525–1529.

Montironi R, Braccishi A, Matera G, Scarpelli M, Pisani E. 1991. Quantitation of prostatic intraepithelial neoplasia. Analysis of nucleolar size, number, and location. Pathol Res Pract 187:307–314.

Pressman N. 1976. Markovian analysis of cervical cell images. J Histochem Cytochem 24:138–144.

Yang P, Huang GS, Zhu AS. 1990. Role of nucleolar organizer regions in differentiating malignant from benign tumors of the colon. J Clin Pathol 43:235–238.